

# Proton and deuteron mass radii from near-threshold $\phi$ -meson photoproduction

Rong Wang,<sup>1,2,\*</sup> Wei Kou,<sup>1,2,†</sup> Chengdong Han,<sup>1,2,‡</sup> Jarah Evslin,<sup>1,2,§</sup> and Xurong Chen<sup>1,2,3,¶</sup>

<sup>1</sup>*Institute of Modern Physics, Chinese Academy of Sciences, Lanzhou 730000, China*

<sup>2</sup>*University of Chinese Academy of Sciences, Beijing 100049, China*

<sup>3</sup>*Guangdong Provincial Key Laboratory of Nuclear Science, Institute of Quantum Matter, South China Normal University, Guangzhou 510006, China*

(Dated: August 10, 2021)

We analyze the exclusive  $\phi$ -meson photoproduction on both hydrogen and deuterium targets based on the published data of CLAS, SAPHIR and LEPS collaborations. A dipole-form scalar gravitational form factor is applied to describe the  $|t|$ -dependence of the differential cross section. From the precise CLAS data of wide  $|t|$  range, we find that the proton and deuteron mass radii are  $0.62 \pm 0.09$  fm and  $1.94 \pm 0.45$  fm respectively. The coherent and near-threshold quarkonium photoproduction seems to be sensitive to the radius of the hadronic system. The vector-meson-dominance model together with a low-energy QCD theorem well describe the data of the near-threshold  $\phi$  photoproduction on the hadronic systems.

Hadronic matter accounts for nearly all the mass of the visible universe. However many mysteries remain concerning hadron structure, such as how the hadron mass, spin and pressure are fixed by strong interactions of the quarks and gluons inside [1–10]. The inside of a hadron is governed by quantum chromodynamics (QCD) theory. In particular, the strong force carrier in QCD, the gluon, is believed to play a dominant role in determining the basic properties of the proton, such as its mass. X. Ji found that the proton mass scale is fixed by the QCD quantum trace anomaly [1–3, 11–14].

Now the proton mass radius is the subject of heated discussions. This mass radius characterizes how the mass is distributed inside the proton, namely the mass density distribution. Experimentally, the form factors as a function of momentum transfer ( $q$ ) are measured in elastic scattering processes, which correspond to the Fourier transforms of the various density distributions. Theoretically, the mass radius of a hadron can be defined in terms of the scalar gravitational form factor (GFF)  $G(t = q^2)$ , the form factor of the trace of the QCD energy-momentum tensor, in a nonrelativistic and weak gravitational field approximation [15]. Similar to the definition of the charge radius, the mass radius is defined as the derivative of the form factor at zero momentum transfer [15, 16],

$$\langle R_m^2 \rangle \equiv \frac{6}{M} \frac{dG(t)}{dt} \Big|_{t=0}, \quad (1)$$

with  $G(0) = M$ .

Following the proposal of D. Kharzeev [15, 17–19], we describe the near-threshold cross section for heavy quarkonium photoproduction using the QCD Van der

Waals force of leading-twist gluon operators derived from a QCD low energy theorem and a vector-meson-dominance (VMD) model. The theoretical uncertainties are argued to be under control in the nonrelativistic limit. The differential cross section for quarkonium photoproduction in the small- $|t|$  region and near the production threshold can be described with the scalar GFF  $G(t)$  [15], which is written as,

$$\frac{d\sigma}{dt} \propto G^2(t). \quad (2)$$

Therefore the near-threshold quarkonium photoproduction data is sensitive to the GFF and the mass distribution. With this theoretical framework and the dipole form of GFF,  $G(t) = M/(1 - t/m_s^2)^2$ , the mass radius of the proton has been extracted from vector meson production data on the hydrogen targets [20].

The  $\phi$  vector meson is a typical quarkonium which do not has the same type of quark of the proton valence components. Thus the  $\phi$  meson interacts with the proton via the gluon exchanges described by the low energy QCD theorem mentioned above in the elastic scattering process. An interesting question is whether or not the scalar GFF is also applicable to the near-threshold quarkonium production on the atomic nucleus (such as the deuteron). The CLAS and LEPS collaborations have measured the coherent  $\phi$ -photoproduction cross sections on hydrogen and deuterium targets [21–24]. Due to the high luminosity of the accelerator and the large acceptance of the CLAS spectrometer, the CLAS data is of high precision over a wide  $|t|$  range [21, 22]. SAPHIR collaboration also has measured the  $\phi$ -photoproduction on the hydrogen target near the reaction threshold [25]. These coherent  $\phi$ -photoproduction data provide an excellent opportunity to determine the mass radii of the proton and the deuteron, and to examine the scalar GFF interpretation of the quarkonium production mechanism in the nonperturbative region.

In this paper, we present simultaneous analyses of the proton mass radius and the deuteron mass radius using CLAS, SAPHIR and LEPS data, following the previous

\* rwang@impcas.ac.cn

† kouwei@impcas.ac.cn

‡ chdhan@impcas.ac.cn

§ jarah@impcas.ac.cn

¶ xchen@impcas.ac.cn

study on the proton mass radius [15, 20]. The systematic uncertainty from varying the  $|t|$  range of the fit is also investigated.

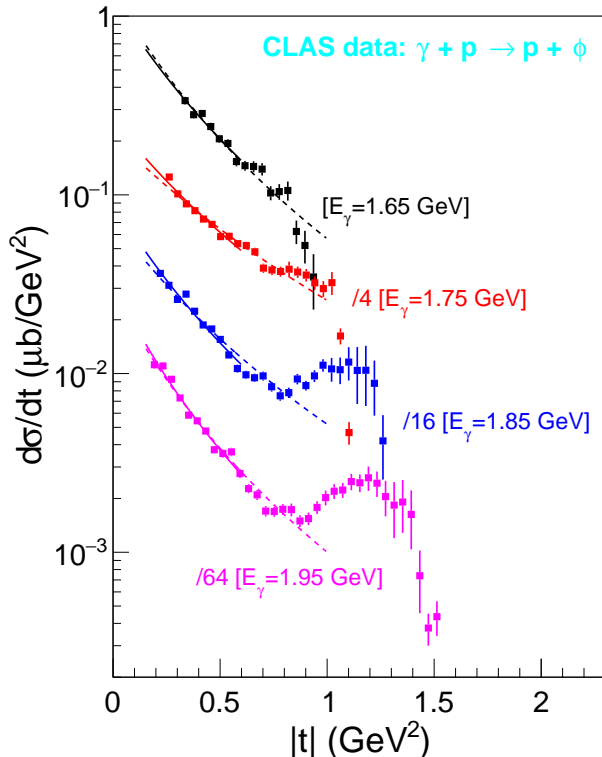


FIG. 1. The differential cross sections of near-threshold  $\phi$  photoproduction on a hydrogen target ( $\gamma p \rightarrow \phi p$ ) from CLAS [21]. Only the statistical errors are presented. Some of the cross sections are scaled by factors indicated in the figure. The dashed curves show the fits in the  $|t|$  range from 0.15  $\text{GeV}^2$  to 1  $\text{GeV}^2$ . The solid curves show the fits in the  $|t|$  range from 0.15  $\text{GeV}^2$  to 0.6  $\text{GeV}^2$ .

TABLE I. The proton mass radii at different photon energies determined from the  $t$ -slopes of the differential cross sections from CLAS, extrapolated to  $t = 0 \text{ GeV}^2$ .

$E_\gamma$ (GeV)	1.65	1.75	1.85	1.95
$R_m^p$ (fm)	$0.62 \pm 0.09$	$0.72 \pm 0.05$	$0.89 \pm 0.04$	$0.89 \pm 0.05$

Fig. 1 shows the CLAS collaboration's near-threshold differential cross section data for  $\phi$  photoproduction on the proton. It has been suggested that the  $|t|$ -dependence of the differential cross section is described by the scalar GFF of the proton. Some fits based on Eq. (2) are shown in the figure. The differential cross section data are well reproduced by the dipole form of the scalar GFF. However in the large- $|t|$  region, approaching  $|t|_{\text{max}}$ , we see the cross section rising with  $|t|$ . This behavior in the large- $|t|$  region may be due to the direct  $\phi$ -radiation

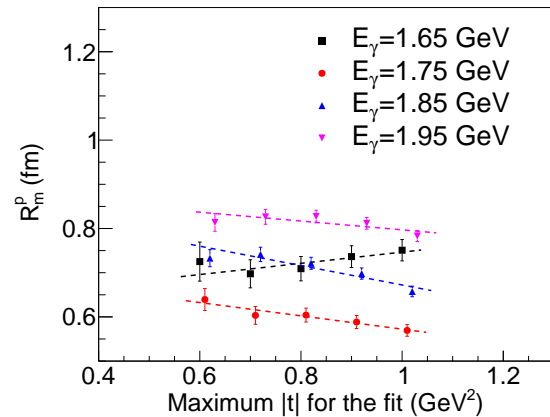


FIG. 2. The proton mass radius as a function of the maximum  $|t|$  in the fitting range, extracted from CLAS data. To avoid overlaps of the data points, the data points at 1.75 GeV, 1.85 GeV, and 1.95 GeV are shifted to the right by 0.01  $\text{GeV}^2$ , 0.02  $\text{GeV}^2$  and 0.03  $\text{GeV}^2$  respectively. The dashed lines display the linear fits of the data.

contributions from  $u$ -channel and  $s$ -channel with  $\phi NN$  coupling or  $\phi NN^*$  coupling [26–33].

In order to avoid such  $u$ -channel or  $s$ -channel contamination, we narrow the fitting range of  $|t|$  towards the small- $|t|$  region. We studied the fits restricted in quite different  $|t|$  ranges carefully, as the CLAS data covers a wide  $|t|$  range and of high precision. To understand the effect of the large- $|t|$  data on the extraction of the scalar GFF, we perform a series of fits excluding the large- $|t|$  data requiring  $|t| < 0.6 \text{ GeV}^2$ ,  $|t| < 0.7 \text{ GeV}^2$ ,  $|t| < 0.8 \text{ GeV}^2$ ,  $|t| < 0.9 \text{ GeV}^2$ , and  $|t| < 1.0 \text{ GeV}^2$  respectively. With each fit, we extract the parameterized scalar GFF and by calculating the derivative at  $t = 0 \text{ GeV}^2$  we find the mass radius. The obtained proton mass radii from these fits are shown in Fig. 2, as a function of the cut at large  $|t|$ . We find that, beneath 1  $\text{GeV}^2$ , the extracted mass radius does not depend strongly on the choice of large- $|t|$  cut. This is probably because the  $u$ -channel or  $s$ -channel contribution only dominates in the large- $|t|$  region where the error bars are comparatively large [27–33]. Therefore the large- $|t|$  data hardly affects the fits. The uncertainty from varying the fitting range of  $|t|$  is of the same order as the statistical uncertainty in the data.

With the linear extrapolations of the dependence on the fitting range shown in Fig. 2, we provide the mass radii in Table I. We see that the extracted mass radius depends weakly on the energy of the incident photon. Since the formalism based on the GFF works mainly in the low energy limit, the reliable mass radius should be given by the data closest to the production threshold. Hence, the mass radius of the proton should be  $0.62 \pm 0.09 \text{ fm}$ , as determined from the  $\phi$  photoproduction data at  $E_\gamma = 1.65 \text{ GeV}$ .

The proton mass radius from the proton data of LEPS collaboration is provided in the previous analysis, which is  $0.67 \pm 0.1$  in average [20]. Though with fewer data

points and larger statistical uncertainties, SAPHIR collaboration has also measured the near-threshold  $\phi$  photo-production on the proton two decades ago [25]. The differential cross section data of SAPHIR are shown in Fig. 3. From the fits of dipole GFF, the SAPHIR data give the proton mass radii to be  $0.69 \pm 0.08$  fm and  $0.59 \pm 0.04$  fm at  $E_\gamma = 1.7$  GeV and  $E_\gamma = 1.95$  GeV, respectively. The CLAS, LEPS and SAPHIR data are consistent with each other.

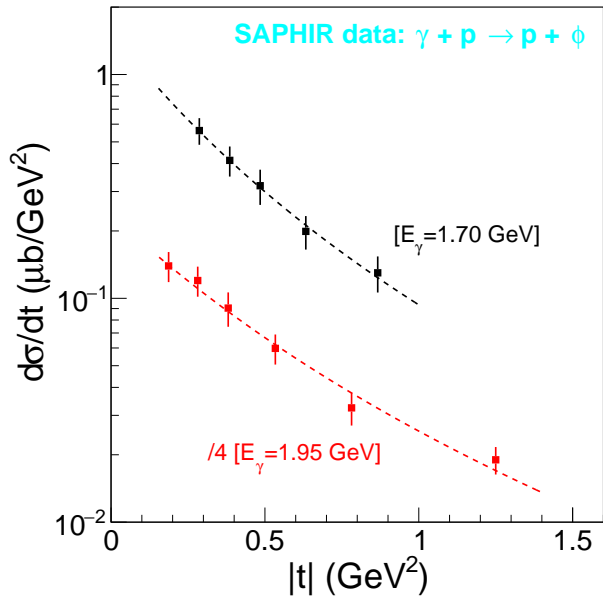


FIG. 3. The differential cross sections of coherent  $\phi$  photo-production on proton near threshold ( $\gamma p \rightarrow \phi p$ ) from SAPHIR [25]. Only the statistical errors are presented. The cross-section data at  $E_\gamma = 1.95$  GeV is divided by 4, as indicated in the figure. The dashed curves show the fits of scalar GFF.

TABLE II. The deuteron mass radii at different photon energies determined from the  $t$ -slopes of the differential cross sections from CLAS, extrapolated to  $t = 0$  GeV<sup>2</sup>.

$E_\gamma$ (GeV)	[1.6, 2.6]	[2.6, 3.6]
$R_m^d$ (fm)	$1.94 \pm 0.45$	$1.78 \pm 0.38$

TABLE III. The deuteron mass radii at different photon energies determined from the  $t$ -slopes of the differential cross sections from LEPS.

$E_\gamma$ (GeV)	1.82	1.92	2.02
$R_m^d$ (fm)	$11.7 \pm 4.2$	$1.80 \pm 0.43$	$2.08 \pm 0.30$

In the following, we perform a similar analysis on the deuteron data. First, we fit the differential cross section

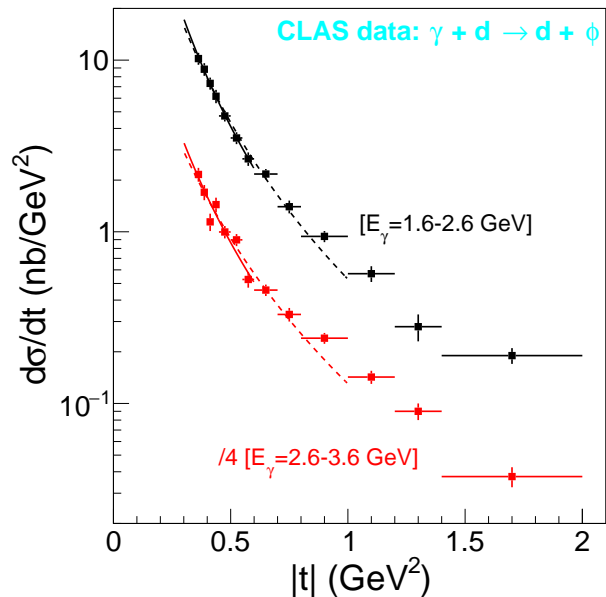


FIG. 4. The differential cross sections of coherent  $\phi$  photo-production on deuteron near threshold ( $\gamma d \rightarrow \phi d$ ) from CLAS [22]. Only the statistical errors are presented. The cross-section data at  $E_\gamma = 3.1$  GeV is divided by 4, as indicated in the figure. The dashed curves show the fits in the  $|t|$  range from 0.3 GeV<sup>2</sup> to 1 GeV<sup>2</sup>. The solid curves show the fits in the  $|t|$  range from 0.3 GeV<sup>2</sup> to 0.6 GeV<sup>2</sup>.

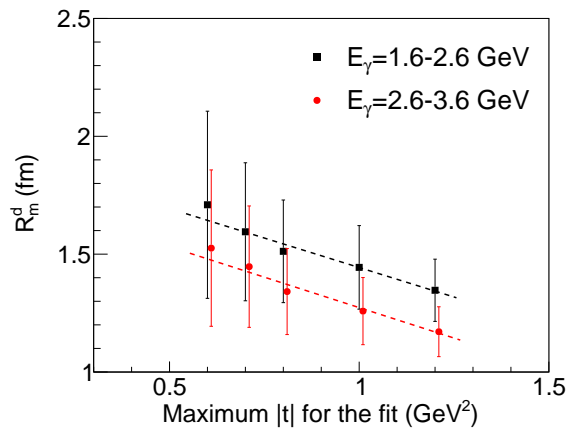


FIG. 5. The deuteron mass radii as a function of the maximum  $|t|$  in the fitting range, extracted from CLAS data. To avoid overlaps of the data points, the data points of the energy bin [2.6, 3.6] GeV are shifted to the right by 0.01 GeV<sup>2</sup>. The dashed lines display the linear fits of the data.

data on the deuteron of CLAS collaboration, using the VMD model and the scalar GFF. Still surprisingly, the dipole form GFF describes well the coherent  $\phi$  photoproduction data on the deuterium target, which is shown in Fig. 4. Second, we study the mass radii of the deuteron extracted from the fits of different  $|t|$  ranges (see Fig. 5). In Fig. 5, we see a relatively stronger dependence on the  $|t|$ -maximum boundary of the fitting range, in

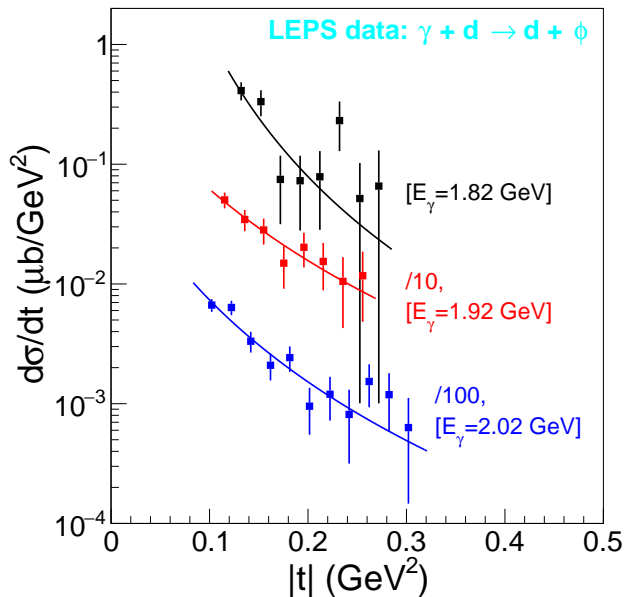


FIG. 6. The differential cross sections of coherent  $\phi$  photoproduction on deuteron near threshold ( $\gamma d \rightarrow \phi d$ ) from LEPS [24]. Only the statistical errors are presented. The cross-section data at  $E_\gamma = 1.92$  GeV and  $E_\gamma = 2.02$  GeV are divided by 10 and 100 respectively, as indicated in the figure. The curves show the fits of scalar GFF.

comparison to the proton data. One reason is probably that there is a stronger contribution from baryonic or nuclear resonances for the deuteron data at the relatively higher photon energy. By linearly extrapolating the fitting range to  $0 \text{ GeV}^2$ , the mass radii of the deuteron at zero momentum transfer are obtained, which are listed in Table II. Finally, as suggested by the most near-threshold data ( $E_\gamma^{\text{aver.}} = 2 \text{ GeV}$ ), the mass radius of the deuteron is estimated to be  $1.94 \pm 0.05 \text{ fm}$ . Strikingly and similar to the proton case, the mass radius of the deuteron is also smaller than the world average of the charge radius of the deuteron (CODATA-2010 average is  $2.1424 \pm 0.0021 \text{ fm}$ ). The high precision data of the deuteron charge radius is from the Lamb shift in the spectrum of the muonic deuteronium, which gives a value of  $2.12562 \pm 0.00078 \text{ fm}$  [34]. For both the proton and the deuteron, the mass radii are about  $0.2 \text{ fm}$  smaller than the charge radii.

LEPS collaboration also measured the near-threshold  $\phi$  photoproduction on the deuteron [24]. The statistical errors are much larger compared to the CLAS data. The

range of the variable  $t$  is also much narrower, which is not good for the extraction of the slope of the differential cross section as a function of  $|t|$ . Nevertheless, the  $|t|$ -dependence of LEPS data also can be described with the dipole form factor. Fig. 6 shows the fits compared to the cross-section data from LEPS. The extracted mass radii of the deuteron at different energies are listed in Table III. The LEPS data is closer to  $t = 0 \text{ GeV}^2$ , and the obtained deuteron mass radius is consistent with the values extracted from CLAS data.

In summary, first, we verified that the VMD model and low-energy QCD theorem suggested by D. Kharzeev accurately describes the near-threshold quarkonium photoproduction. We find that the VMD model and the dipole-form GFF reproduce well the  $|t|$ -dependence of the differential cross section of  $\phi$  photoproduction on both the proton and the deuteron. Nevertheless, there should be more studies on the GFF and the mechanical properties of the hadronic system encompassing more experimental data in the future. Second, the mass radii of the proton and the deuteron are determined from the parameterized GFF extracted from the coherent and near-threshold  $\phi$  photoproduction data from CLAS and LEPS collaborations. The mass radii are found to be smaller than the charge radii for both the proton and the deuteron. Third, the systematic uncertainty of the analysis is briefly investigated. The mass radius extracted from the  $|t|$ -dependence of the cross section is not sensitive to the size of the fitting range as long as  $|t| < 1 \text{ GeV}^2$ . The dependence of the extracted mass radius on the photon energy is weak. Judged by the CLAS data at several near-threshold energies, the model uncertainty from non-at-threshold effects is of the same order as the current statistical uncertainty for both the proton and the deuteron.

To further check the GFFs and the mass distributions of the proton and the nuclei, the measurements of near-threshold photoproduction of  $J/\psi$  and  $\Upsilon$  will be performed at future Electron-Ion Colliders [35–39].

## ACKNOWLEDGMENTS

This work is supported by the Strategic Priority Research Program of Chinese Academy of Sciences under the Grant Number XDB34030301, the CAS Key Research Program of Frontier Sciences QYZDY-SSW-SLH006 and the National Natural Science Foundation of China under the Grant Numbers: 12005266, 11875296 and 11675223.

- 
- [1] X.-D. Ji, Phys. Rev. Lett. **74**, 1071 (1995), arXiv:hep-ph/9410274.  
 [2] X.-D. Ji, Phys. Rev. D **52**, 271 (1995), arXiv:hep-ph/9502213.  
 [3] X. Ji and Y. Liu, (2021), arXiv:2101.04483 [hep-ph].  
 [4] X.-D. Ji, Phys. Rev. D **55**, 7114 (1997), arXiv:hep-

- ph/9609381.  
 [5] X.-D. Ji, Phys. Rev. D **58**, 056003 (1998), arXiv:hep-ph/9710290.  
 [6] X.-D. Ji, Phys. Rev. Lett. **78**, 610 (1997), arXiv:hep-ph/9603249.  
 [7] O. V. Teryaev, Front. Phys. (Beijing) **11**, 111207 (2016).

- [8] M. V. Polyakov, Phys. Lett. B **555**, 57 (2003), arXiv:hep-ph/0210165.
- [9] M. V. Polyakov and P. Schweitzer, Int. J. Mod. Phys. A **33**, 1830025 (2018), arXiv:1805.06596 [hep-ph].
- [10] V. D. Burkert, L. Elouadrhiri, and F. X. Girod, Nature **557**, 396 (2018).
- [11] Y.-B. Yang, J. Liang, Y.-J. Bi, Y. Chen, T. Draper, K.-F. Liu, and Z. Liu, Phys. Rev. Lett. **121**, 212001 (2018), arXiv:1808.08677 [hep-lat].
- [12] R. Wang, J. Evslin, and X. Chen, Eur. Phys. J. C **80**, 507 (2020), arXiv:1912.12040 [hep-ph].
- [13] S. Rodini, A. Metz, and B. Pasquini, JHEP **09**, 067 (2020), arXiv:2004.03704 [hep-ph].
- [14] A. Metz, B. Pasquini, and S. Rodini, Phys. Rev. D **102**, 114042 (2020), arXiv:2006.11171 [hep-ph].
- [15] D. E. Kharzeev, (2021), arXiv:2102.00110 [hep-ph].
- [16] G. A. Miller, Phys. Rev. C **99**, 035202 (2019), arXiv:1812.02714 [nucl-th].
- [17] D. Kharzeev, Proc. Int. Sch. Phys. Fermi **130**, 105 (1996), arXiv:nucl-th/9601029.
- [18] D. Kharzeev, H. Satz, A. Syamtomov, and G. Zinovjev, Eur. Phys. J. C **9**, 459 (1999), arXiv:hep-ph/9901375.
- [19] H. Fujii and D. Kharzeev, Phys. Rev. D **60**, 114039 (1999), arXiv:hep-ph/9903495.
- [20] R. Wang, W. Kou, Y.-P. Xie, and X. Chen, Phys. Rev. D **103**, L091501 (2021), arXiv:2102.01610 [hep-ph].
- [21] H. Seraydaryan *et al.* (CLAS), Phys. Rev. C **89**, 055206 (2014), arXiv:1308.1363 [hep-ex].
- [22] T. Mibe *et al.* (CLAS), Phys. Rev. C **76**, 052202 (2007), arXiv:nucl-ex/0703013.
- [23] T. Mibe *et al.* (LEPS), Phys. Rev. Lett. **95**, 182001 (2005), arXiv:nucl-ex/0506015.
- [24] W. C. Chang *et al.*, Phys. Lett. B **658**, 209 (2008), arXiv:nucl-ex/0703034.
- [25] J. Barth *et al.*, Eur. Phys. J. A **17**, 269 (2003).
- [26] E. Anciant *et al.* (CLAS), Phys. Rev. Lett. **85**, 4682 (2000), arXiv:hep-ex/0006022.
- [27] J. M. Laget, Phys. Lett. B **489**, 313 (2000), arXiv:hep-ph/0003213.
- [28] Q. Zhao, B. Saghai, and J. S. Al-Khalili, Phys. Lett. B **509**, 231 (2001), arXiv:nucl-th/0102025.
- [29] A. I. Titov and T. S. H. Lee, Phys. Rev. C **67**, 065205 (2003), arXiv:nucl-th/0305002.
- [30] R. A. Williams, Phys. Rev. C **57**, 223 (1998).
- [31] A. I. Titov, T. S. H. Lee, and H. Toki, Phys. Rev. C **59**, R2993 (1999), arXiv:nucl-th/9812074.
- [32] A. I. Titov, T. S. H. Lee, H. Toki, and O. Streltsova, Phys. Rev. C **60**, 035205 (1999).
- [33] Y.-s. Oh and H. C. Bhang, Phys. Rev. C **64**, 055207 (2001), arXiv:nucl-th/0104068.
- [34] R. Pohl *et al.* (CREMA), Science **353**, 669 (2016).
- [35] R. Abdul Khalek *et al.*, (2021), arXiv:2103.05419 [physics.ins-det].
- [36] A. Accardi *et al.*, Eur. Phys. J. A **52**, 268 (2016), arXiv:1212.1701 [nucl-ex].
- [37] X. Chen, PoS **DIS2018**, 170 (2018), arXiv:1809.00448 [nucl-ex].
- [38] X. Chen, F.-K. Guo, C. D. Roberts, and R. Wang, Few Body Syst. **61**, 43 (2020), arXiv:2008.00102 [hep-ph].
- [39] D. P. Anderle *et al.*, Front. Phys. (Beijing) **16**, 64701 (2021), arXiv:2102.09222 [nucl-ex].